Analysis of Atmospheric Gravity Waves Using the U. S. Radiosonde Data

Ling Wang

GATS

Boulder, Colorado USA

Introduction

- GWs are small- to meso-scale phenomena with global and significant impacts.

- At present, GW source spectra are still poorly constrained by observations and this can lead to large model uncertainties.

- More observations of GWs are still sorely needed.

- The U.S. HVRRD provide multiple years of high vertical resolution wind and temperature in both the lower stratosphere and troposphere over a very wide range of geographic locations. Thus, they are very suitable for constraining GW source spectra observationally.

- A brief review of GW analysis using HVRRD is provided here.

GW perturbations

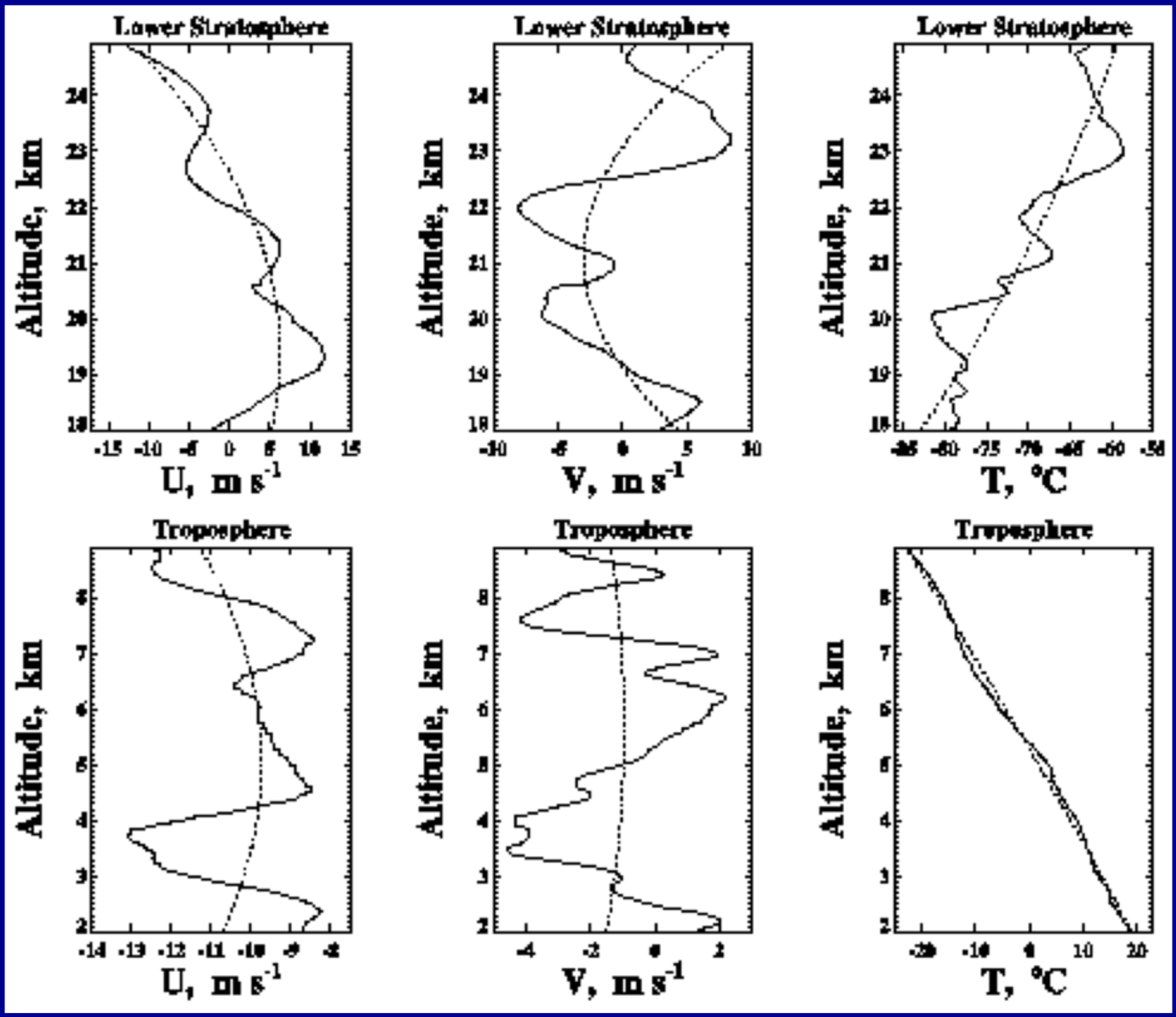

6-second US HVRRD data

The wavelike structures are assumed to be caused by GWs.

Following Allen and Vincent 1995 JGR and Vincent et al. 1997

2nd order polynomial fit is used to represent background -> GW perturbations

Solid lines: U, V, T profiles in LS (18-24.9 km) and Trop (2-8.9 km) over Ponape Island (from Wang and Geller 2003, JGR)

Morphology of GW Et

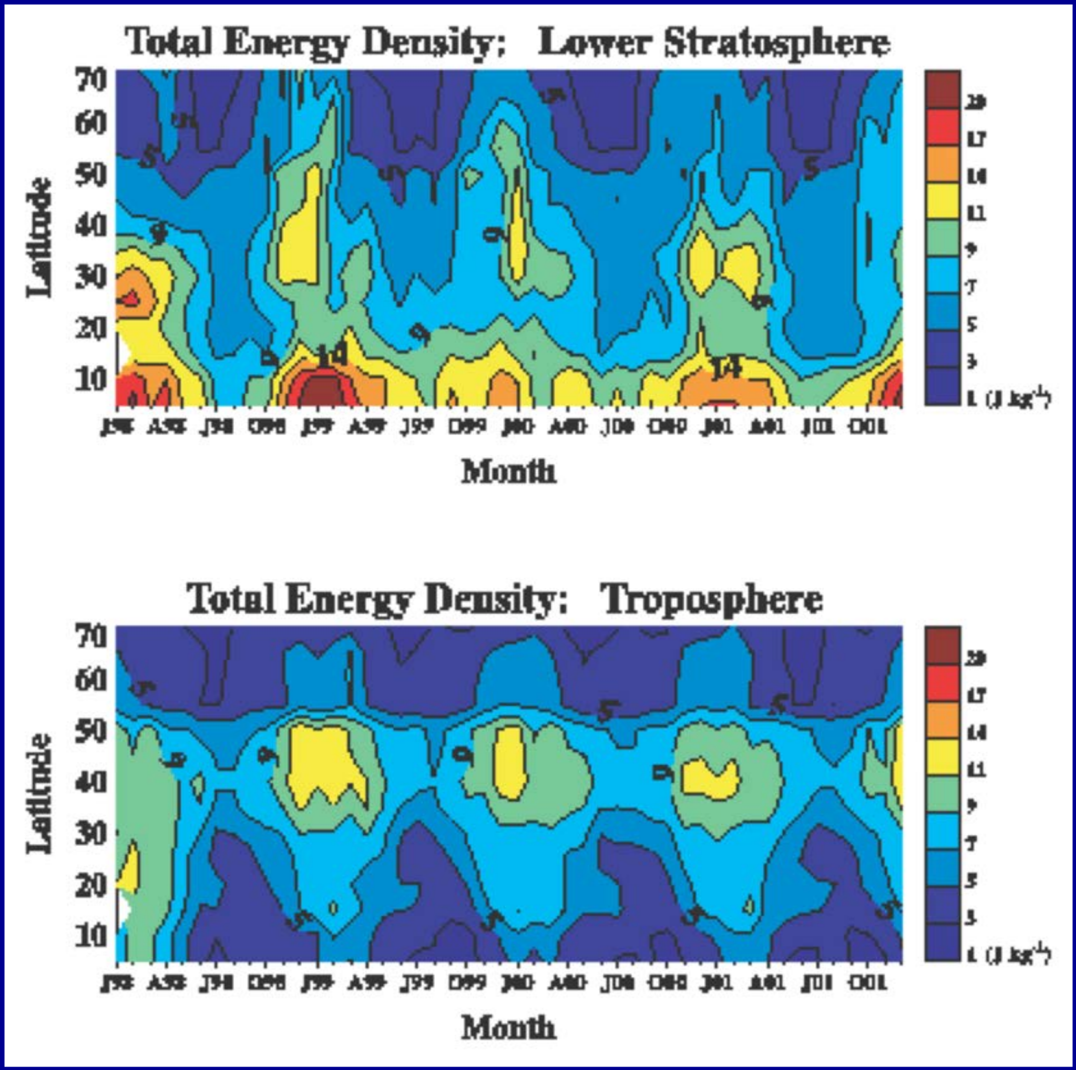

Monthly and zonal mean Et in LS and Tropo during 1998-2001 from US HVRRD (from Wang and Geller 2003, JGR)

$$E_t = KE + PE \simeq \frac{1}{2}\left(\overline{u'^2} + \overline{v'^2} + \frac{g^2\overline{\hat{T}'^2}}{N^2}\right)$$

Et decreases with increasing latitude in LS and maximizes at 40N in Trop.

Et is larger in winter in both Trop and LS.

Interannual variation is seen in both LS and Trop.

Possible links with ENSO and QBO

Morphology of GW Et

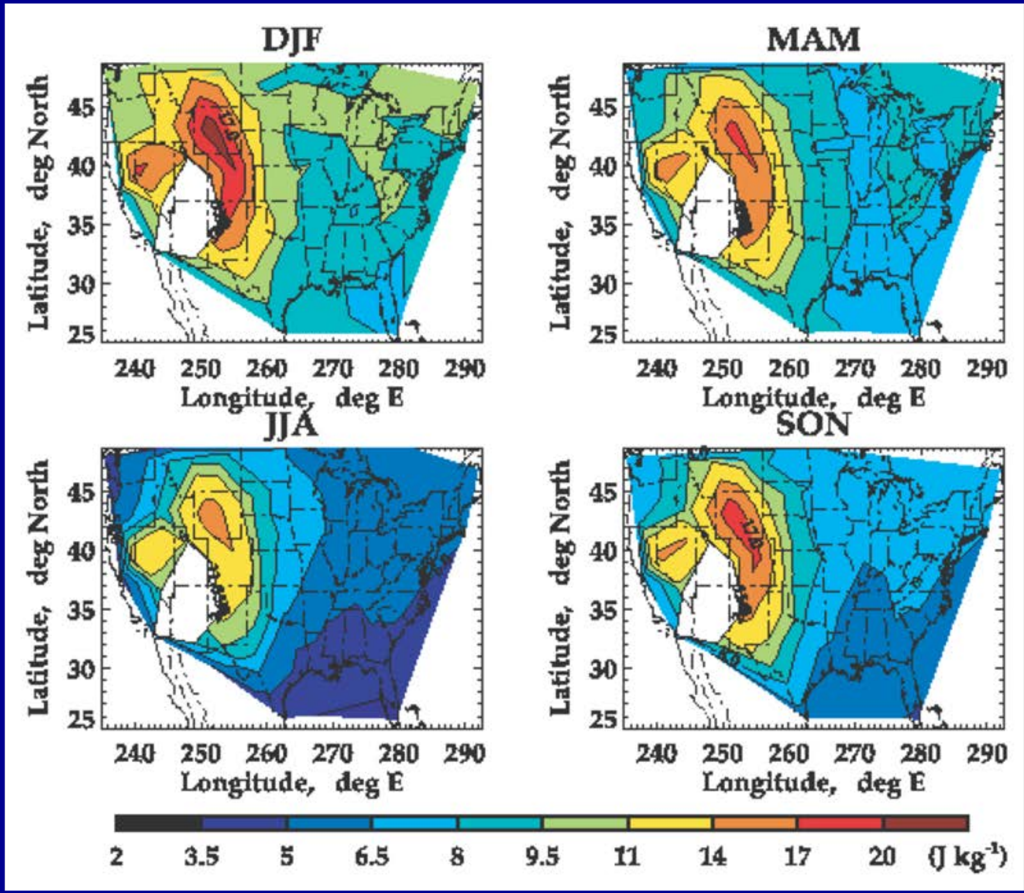

Clear evidence of topographic excitation of GWs over the Rocky Mountains & Appalachian mountains

Notable absence of convective GWs in JJA

Four-year (1998-2001) averaged seasonal mean Et in troposphere (from Wang and Geller 2003, JGR)

GW Intrinsic Frequency

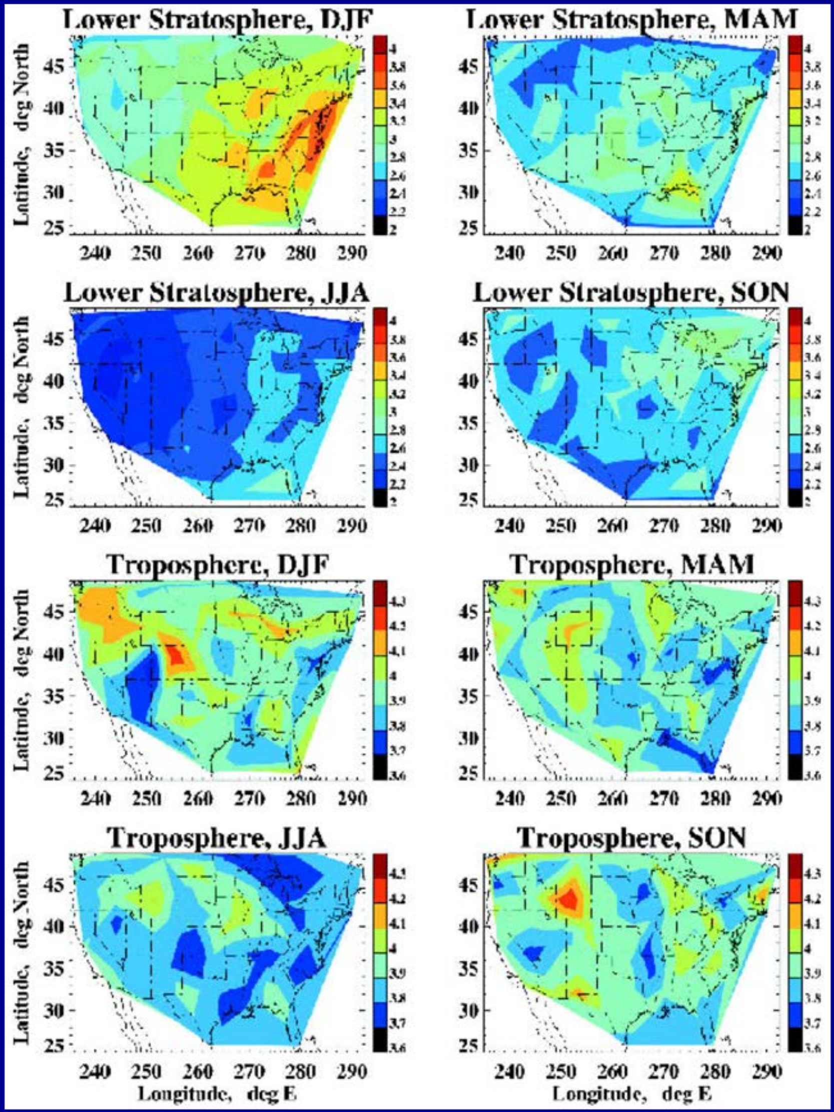

Axial ratio of wind perturbation hodograph (the Stokes parameters method) → omega/f.

Omega/f ~ 4 in Trop, ~ 2.4-3 in LS, i.e., *inertio-gravity waves*!

In LS, omega is larger in winter than in summer, consistent with variation of background wind. It is smaller over western U.S.

In Trop, geographic and seasonal variations of omega are more complicated, but it is still higher in winter than in summer.

Five-year (1998-2002) averaged seasonal mean of intrinsic frequency/f in LS and Trop (from Wang etal 2005, JAS)

GW Vertical Wavelength

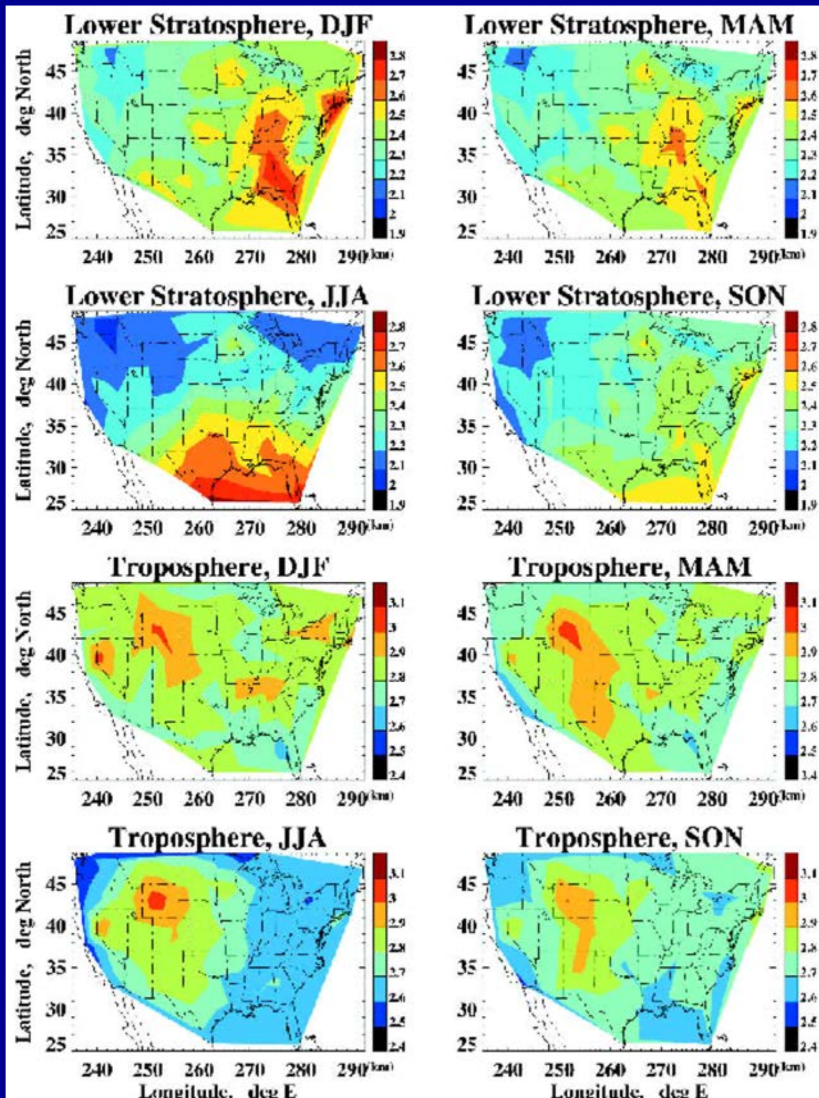

Energy-weighted mean vertical wavenumber of the normalized T' → vertical wavelength Lz

Distinctive spatial and seasonal variations of Lz

Lz is longer over southeast U.S. in LS; but it maximizes over the Rockies in Trop.

Lz is longer in winter than in summer, except south of ~ 35N in LS.

Lz is slightly longer in Trop than in LS.

Five-year (1998-2002) averaged seasonal mean of vertical wavelength in LS and Trop (from Wang etal 2005, JAS)

GW Horizontal Wavelength

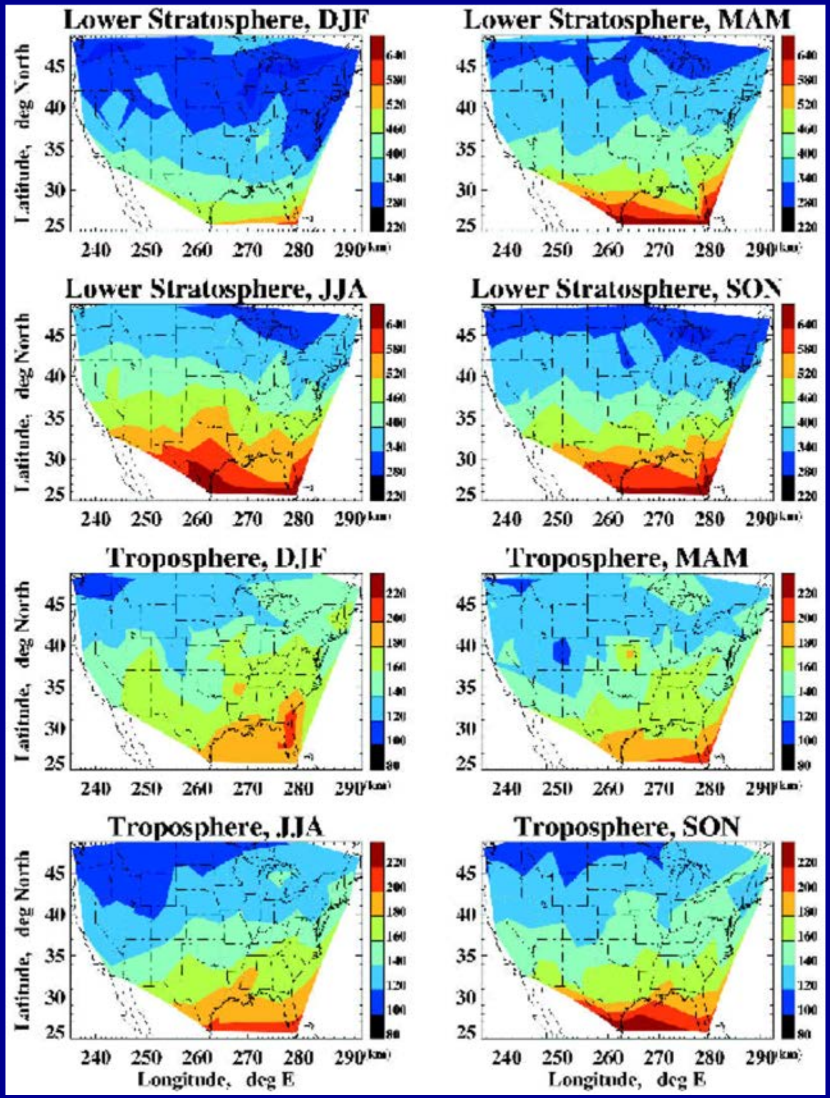

Horizontal wavelength Lh is determined from intrinsic frequency and vertical wavelength using GW dispersion relation.

Lh decreases with increasing latitudes.

Lh is longer in LS than in Trop

Five-year (1998-2002) averaged seasonal mean horizontal wavelength in LS and Trop (from Wang etal 2005, JAS)

Fraction of GW Upward Propagation

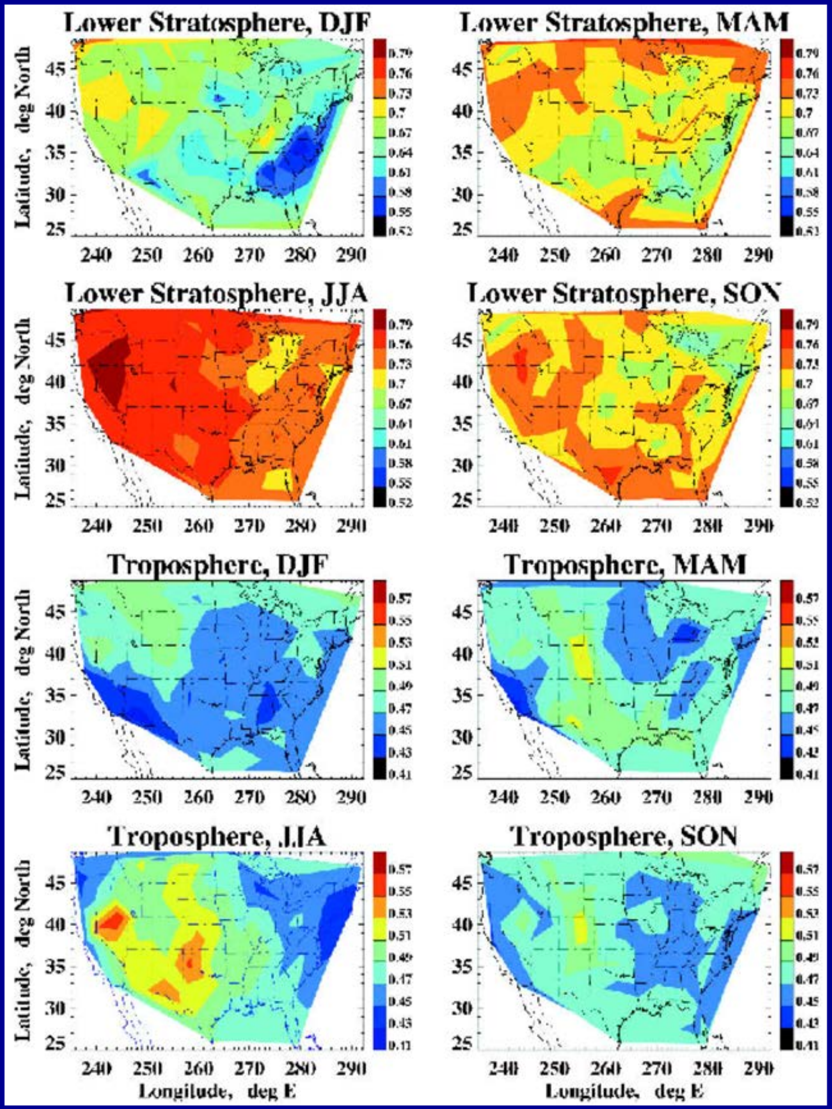

Five-year (1998-2002) averaged seasonal mean of fraction of upward energy propagation in LS and Trop (from Wang etal 2005, JAS)

The rotary-spectral technique is used to decompose wind perturbation into anticlockwise and clockwise components → fraction of upward energy propagation

~ 75% in LS, ~ 50% in

Greater fraction over the windward (lee) side of the Rockies in LS (Trop)

Greater fraction in summer than in winter

GW Horizontal Propagation Direction

Orientation of major axis of hodograph + phase diff between u’, v’ and T’
→ GW horizontal propagation direction

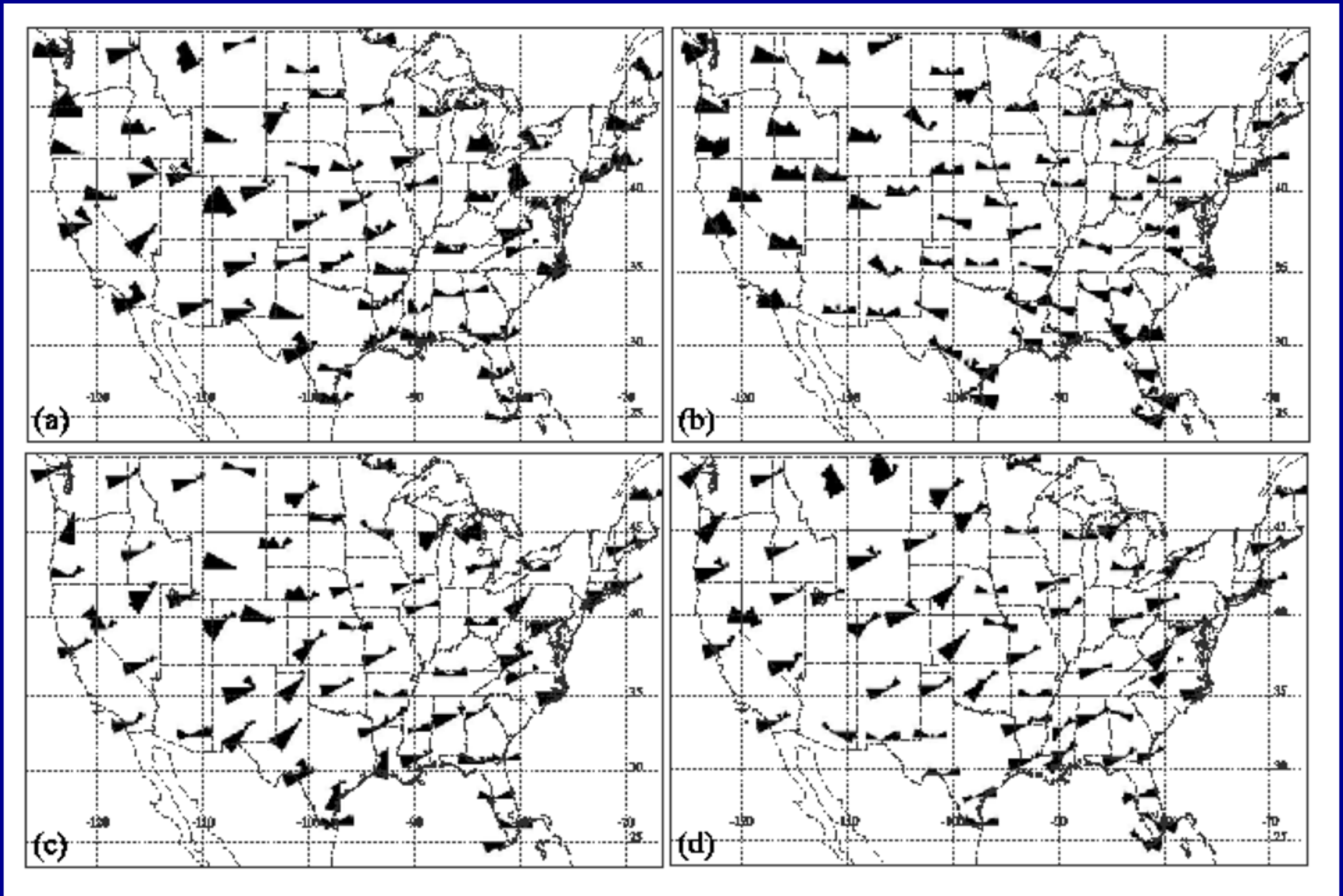

8 yrs of HVRRD (1998-2005) analyzed

predominantly westward in most of contiguous U.S. except for some eastern and Florida stations in summer

nearly isotropic propagation for some midwest stations

8-year (1998-2005) averaged energy-weighted propagation direction for (a) winter LS; (b) summer LS; (c) winter Trop; & (d) summer Trop (from Gong et al. 2008, JGR)

GW Horizontal Propagation Direction

GWs propagate predominantly eastward for the west tropical Pacific stations

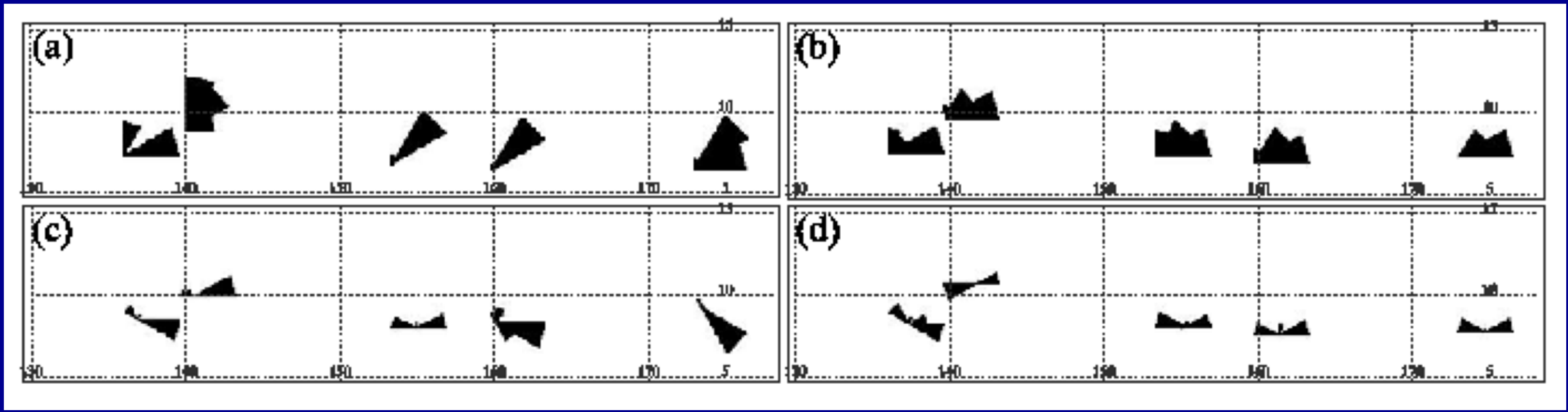

Propagation directions for west tropical Pacific stations for (a) winter LS; (b) summer LS; (c) winter Trop; and (d) summer Trop (from Gong et al. 2008, JGR)

Fitting GW Source Spectra

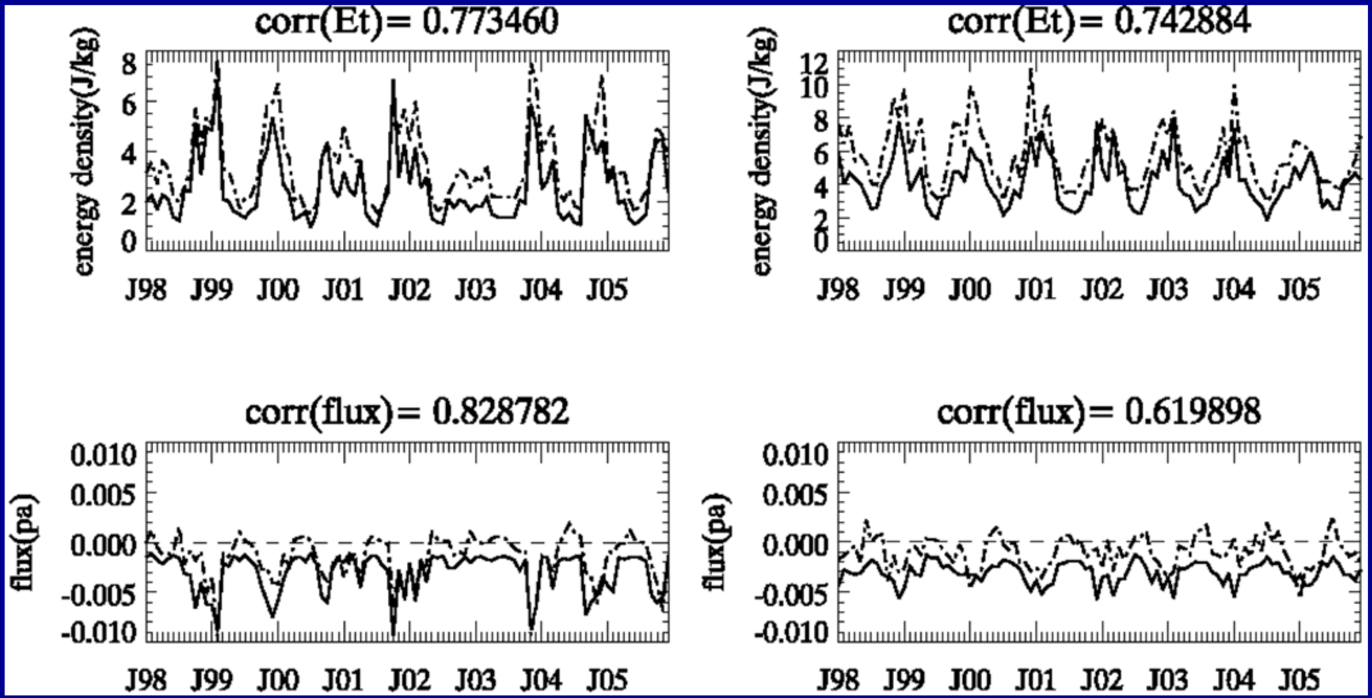

Following Alexander and Vincent 2000, Gong et al. 2008 compared monthly time series of KE & momentum flux in the lower stratosphere obtained from ray-tracing a bunch of specified GW source spectra with "observed" time series of KE & momentum flux for each station to obtain "best fits" of GW source spectra.

Two examples of "best fits". L: King Salmon, AK; R: Blacksburg, VA. Solid: simulation; Dashed: "observation"; Top: KE; Bottom: momentum flux (from Gong et al. 2008, JGR)

Fitting GW Source Spectra

Results

- “Best fit” source spectra are obtained for 61 of the 85 stations tested.
- All “best fit” sources found are anisotropic, with most of the momentum flux directed upstream of the dominant wind direction.
- A source spectrum type representing convection works well at lower latitudes.
- The central U.S. and North American monsoon region are difficult to get “best fits”.

(from Gong et al. 2008, JGR)

GW Vertical Fluctuation Energy

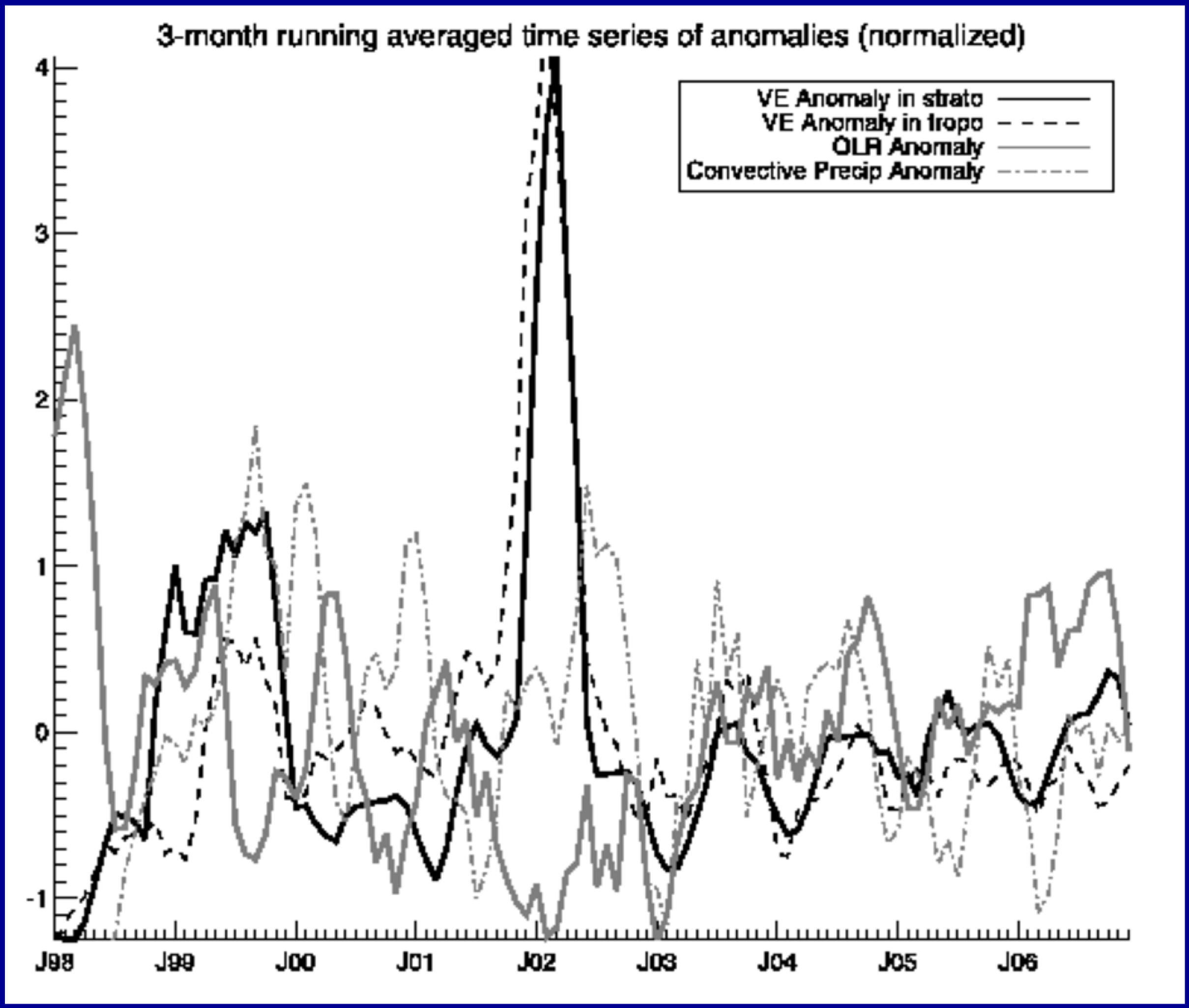

Following Reeder et al. 1999 and Lane et al. 1999, Gong and Geller 2010 derive vertical velocity perturbation and vertical fluctuation energy, VE, from the balloon ascent rate.

9 years (1998-2006)

In the tropics, VE in both LS and Trop are highly correlated with convection.

Normalized monthly means of VE anomalies in LS, Trop, OLR, and convective precipitation at surface over Marshall Island (171.38E, 7.08N) (from Gong and Geller 2010, JGR)

Morphology of GW Vertical Fluctuation Energy

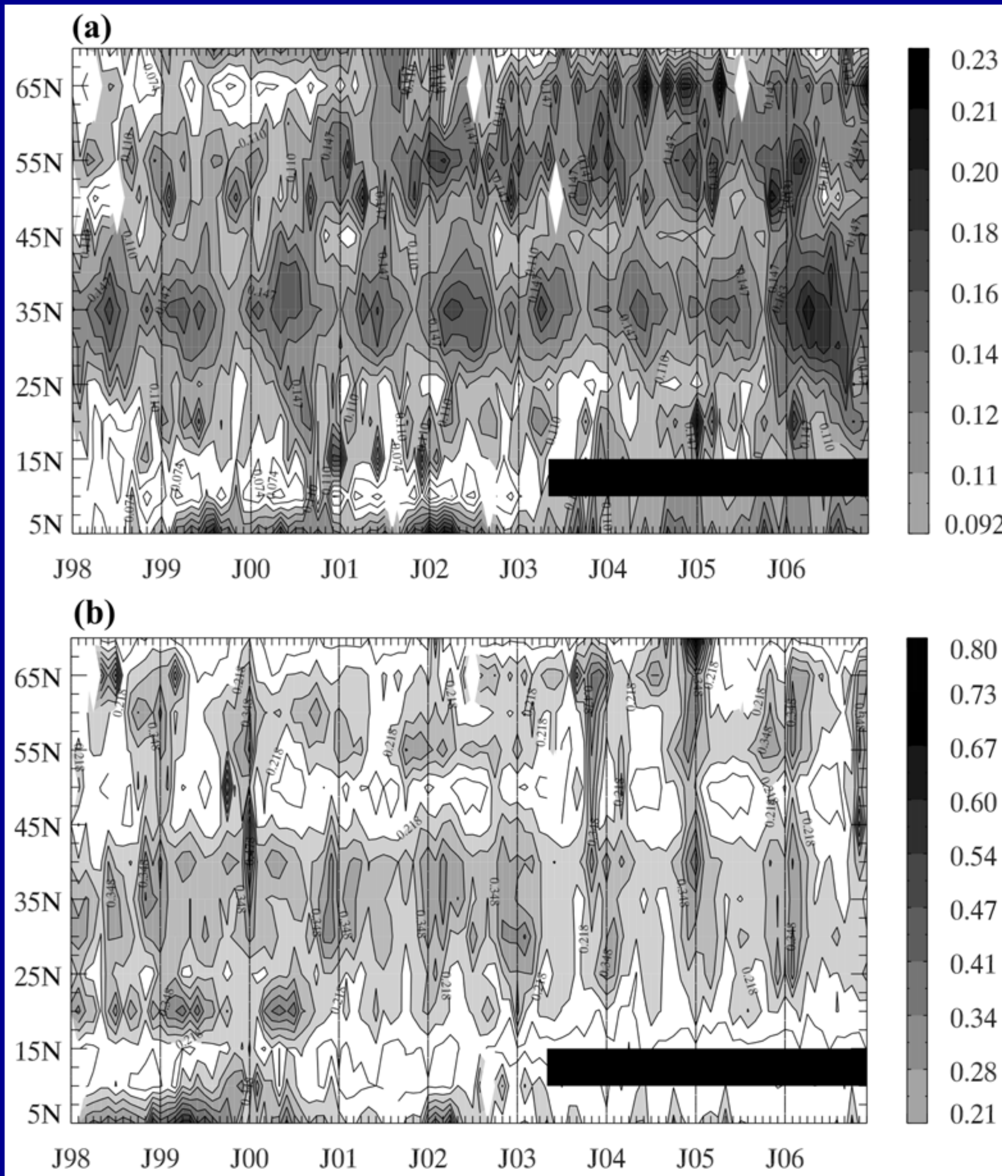

Month-latitude contours of VE in (a) Trop and (b) LS (from Gong and Geller 2010, JGR)

In Trop, VE maximizes at mid-latitudes in summer when convective activities are strongest.

In LS, VE maximizes in winter, with much weaker peaks in summer.

The difference between LS and Trop VE seasonal variations indicate that most of the convectively forced GWs at mid-latitudes do not propagate up to LS.

GW KE, PE, and VE

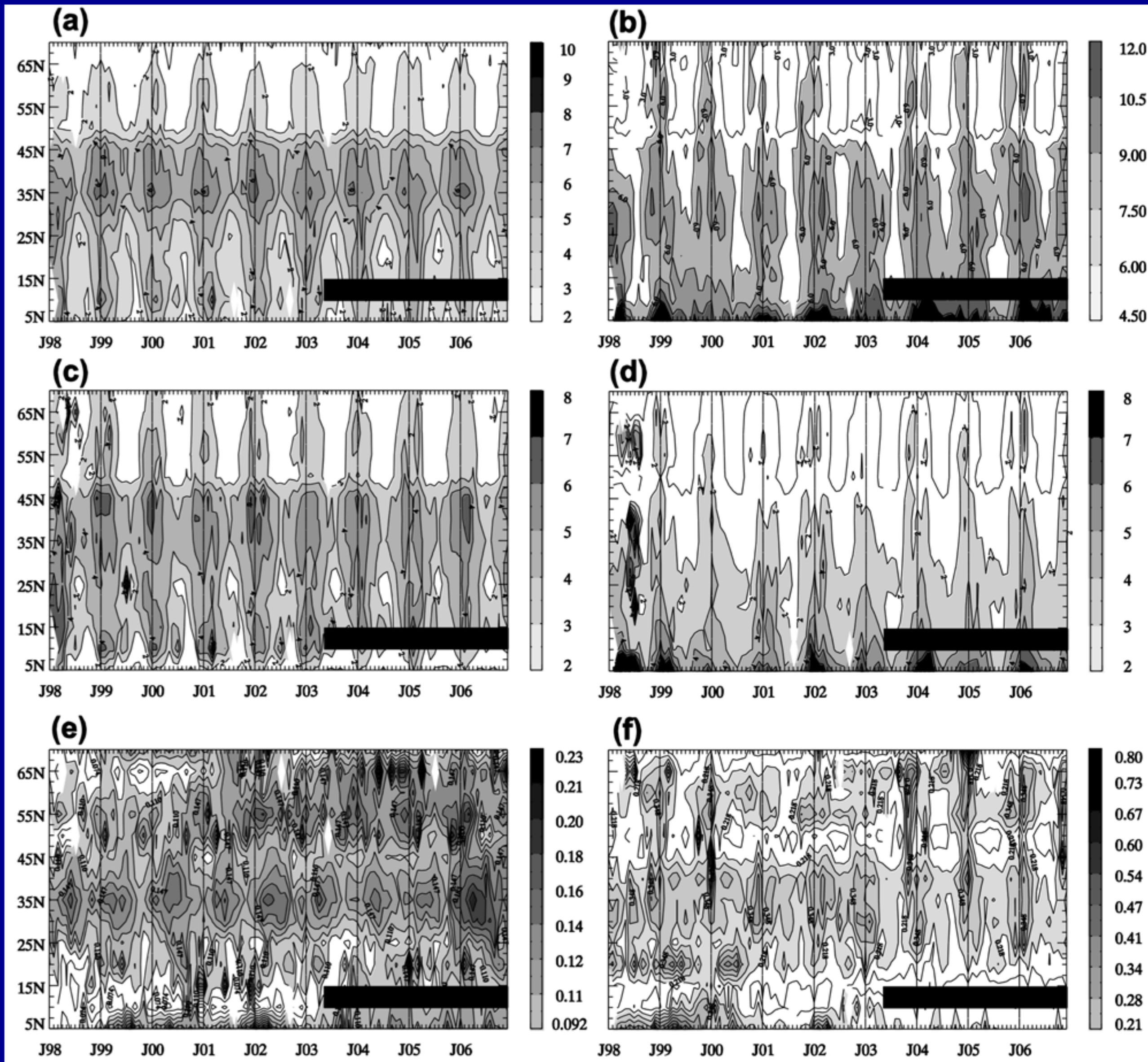

KE, PE and VE show quite different variations in time and latitude.

This is because they are sensitive to different part of the GW spectrum.

KE has the most sensitivity to low frequency GWs.

VE has the most sensitivity to higher frequency GWs.

PE is in between.

9-year (1998-2006) monthly mean KE (upper), PE (middle), & VE (lower) in Trop (left) & LS (right) (from Geller and Gong 2010, JGR)

GW analysis of U.S. HVRRD (Zhang et al. 2012, 2013 JGR)

"Broad spectral method"

1. Monthly mean is removed.
2. A high-pass filter is applied to the residual components of the raw data.
3. The filtered data is smoothed by a Hanning window.

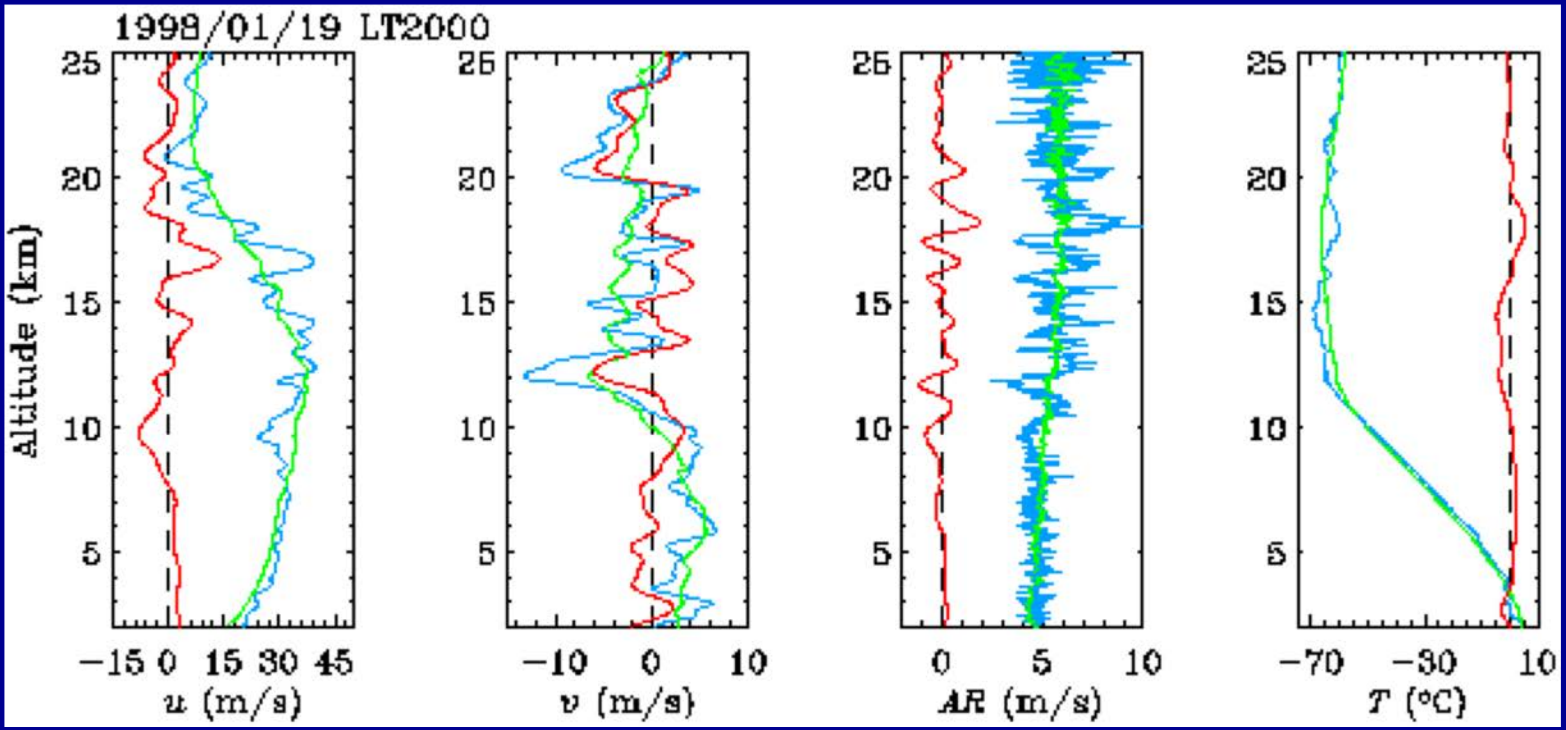

Background may change significantly within a month!

Examples of original (blue), background (green), and GW perturbation (red) profiles over Miramar, CA (32.87N, 117.13W) (from Zhang et al. 2012 JGR)

GW analysis of U.S. HVRRD (Zhang et al. 2012, 2013 JGR)

They also use a different approach to estimate monthly mean KE, PE, and VE; they average KE, PE, and VE in time only -> vertical profiles are derived

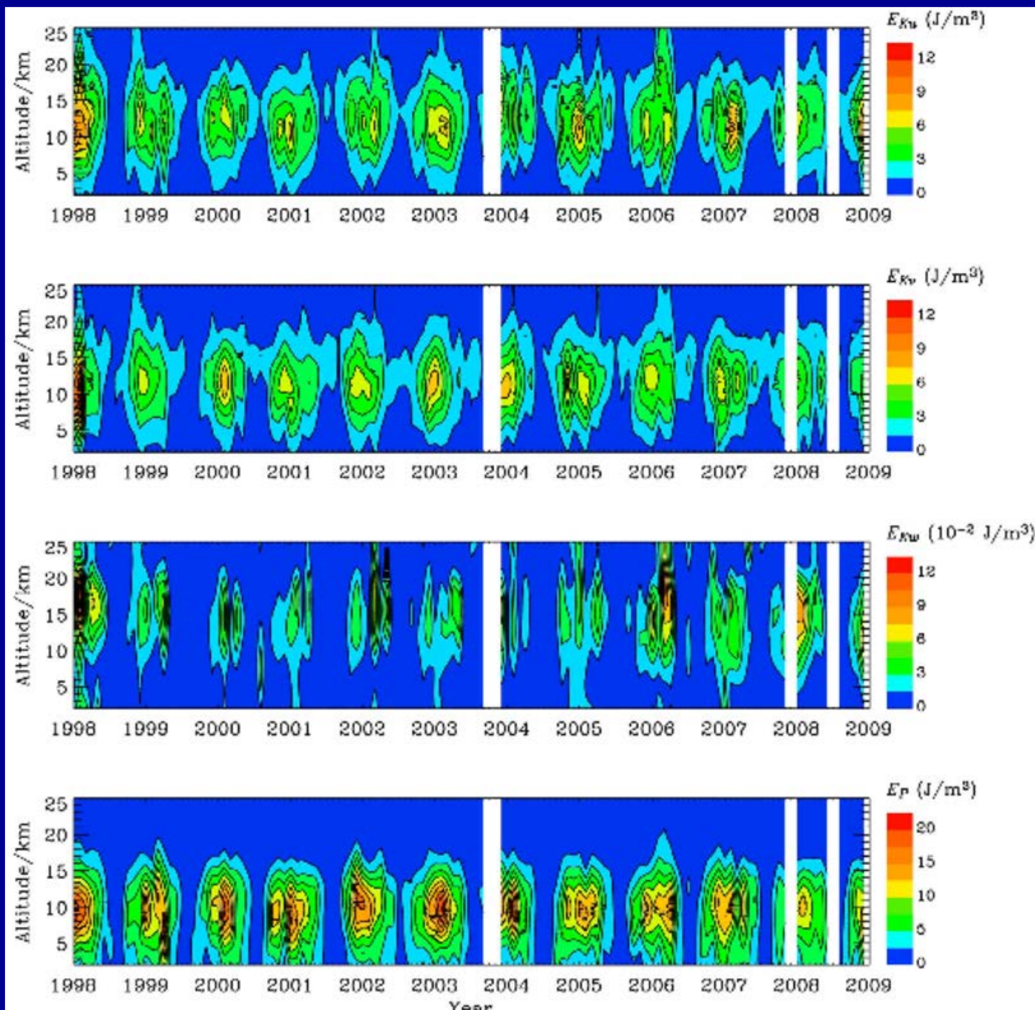

11-year (1998-2008)

Energies maximize at ~ 10 km except for VE which maximizes at ~ 15 km.

They all maximize in winter and minimize in summer.

Seasonal variation of VE in Trop differs from previous studies

Monthly mean KEx, KEy, VE, & PE over Miramar, CA (from Zhang et al. 2012 JGR)

GW analysis of Chinese HVRRD

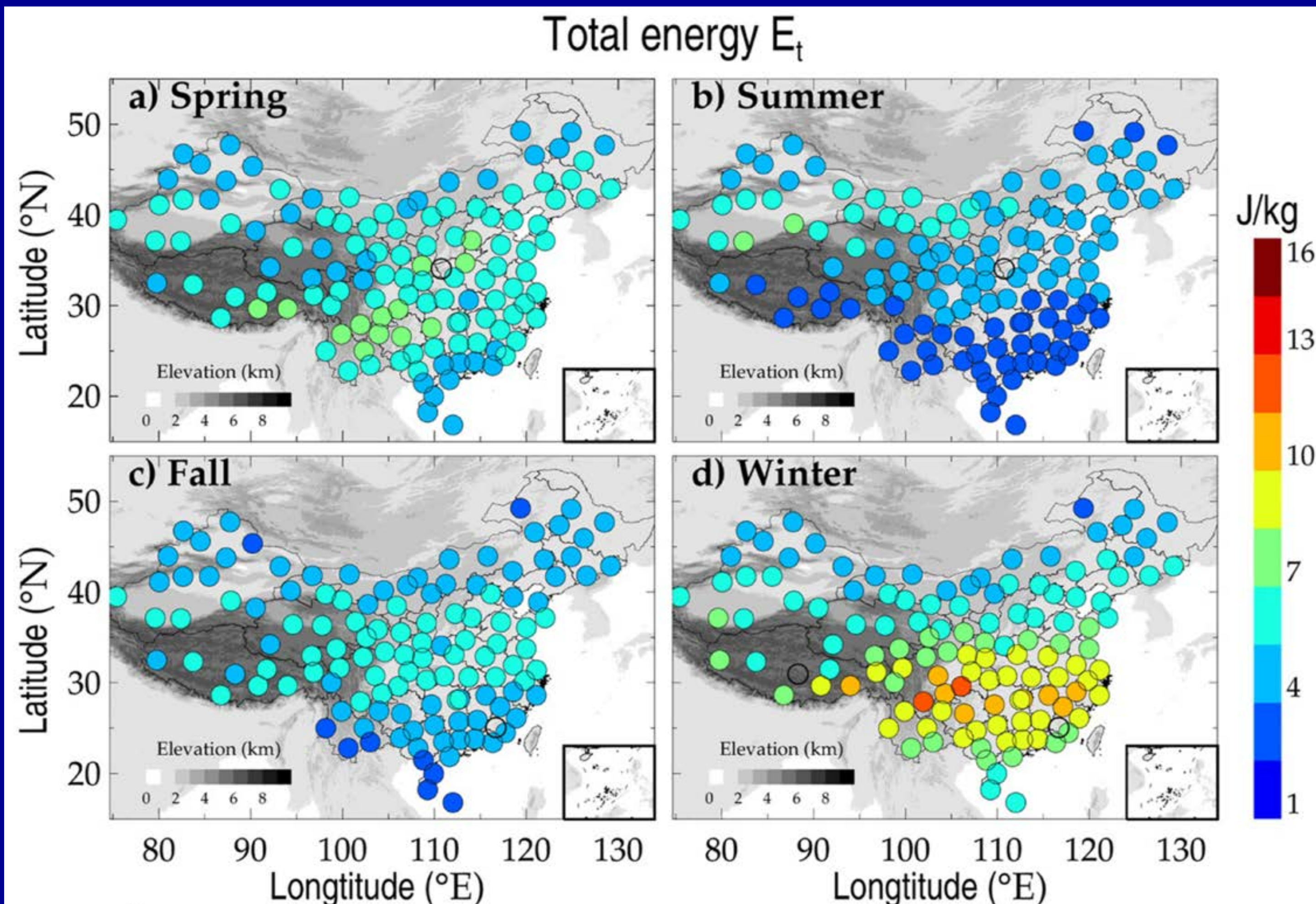

Seasonal mean tropospheric Et (from Zhang et al. 2022 JGR)

1-second data
from 120 stations

During 2016-2019

Z: 2 km – 2/3 TPH

"Broad spectral method" and 0.3-5.5 km passband was used

Tropopause height can vary significantly within a month.

Intercomparison with other data?

Other GW Observations

- There are other types of measurements, both *in situ* and remote sensing (e.g., satellite, rocket, radar, aircraft, lidar), which have been used to study gravity waves.
- Different types of measurements (including among different satellite measurements themselves) may be sensitive to different parts of the gravity wave spectrum.
- Various data analyses can be combined to get a more complete picture and understanding of gravity waves and their source characteristics.

Summary and Concluding Remarks

- The U.S. high vertical resolution radiosonde data are invaluable in obtaining observational constraints for gravity wave source spectra.
- We have learned considerably about the morphology of GW parameters and GW source spectra from analyzing HVRRD during the past few decade and some of the previous studies on this subject have just been reviewed briefly here.
- The analysis can be extended to more stations in the global HVRRD data.

Summary and Concluding Remarks (cont.)

- Additional GW analysis methods can also be applied to HVRRD to obtain more detailed estimates of GW parameters for selected gravity wave events. For example, a combination of wavelet method and the hodograph analysis may be used (e.g., Zink and Vincent 2001 JGR; Wang et al. 2006 AG; Wang and Alexander 2010 JGR).

- The HVRRD GW analysis and GW analyses from other types of measurements (and numerical simulations) can be combined to get a more complete picture and understanding of gravity waves and their sources.